https://doi.org/10.5194/egusphere-2026-6740
Preprint. Discussion started: 11 November 2026
© Author(s) 2026. CC BY 4.0 License.

Meteorological conditions associated with visible CCN and INP perturbations on low clouds at industrial aerosol hot spots

Heido Trofimov, Piia Post, Hannes Keernik, Jorma Rahu, Andres Luhamaa, Margit Aun, Velle Toll

Centre for Climate Research, Institute of Physics, University of Tartu, Tartu, Estonia
Correspondence to: Heido Trofimov (heido.trofimov@ut.ee)

Abstract

Aerosol impacts on clouds remain the most uncertain driver of anthropogenic climate change. Anthropogenic aerosols can brighten liquid-water clouds by serving as cloud condensation nuclei (CCN), but some aerosols also promote glaciation of supercooled liquid-water clouds by serving as ice-nucleating particles (INPs). Conditions favouring these contrasting responses remain poorly understood. Here, we compare meteorological conditions associated with visible CCN and INP perturbations at five isolated industrial aerosol sources in Russia and Canada during 2000–2021. We detect perturbations visually in satellite imagery and characterise the associated conditions using satellite remote sensing and atmospheric reanalysis. At the four sites with both perturbation types, 46 % of liquid-cloud days showed no visible aerosol signal, 33 % showed CCN perturbations and 21 % INP perturbations, with strong seasonality in all three categories. Synoptic-scale circulation strongly influenced whether liquid-phase clouds and visible aerosol perturbations occurred, but separated CCN and INP perturbations only weakly. Relative to climatology, both perturbation types occurred under anomalously high sea level pressure and dry air. INP perturbations occurred in substantially colder environments than CCN perturbations, mainly reflecting their cold-season occurrence and the presence of susceptible supercooled clouds. Several other differences, such as higher static stability during INP perturbations, largely disappeared once seasonality was removed. The CCN-to-INP perturbation ratio differed strongly between sites, with only INP perturbations detected near the cement plant in Volsk. This is consistent with expected differences in emitted aerosol properties and suggests that the properties of emitted aerosols strongly influence whether the CCN or INP effect dominates.

https://doi.org/10.5194/egusphere-2026-6740
Preprint. Discussion started: 11 November 2026
© Author(s) 2026. CC BY 4.0 License.

1 Introduction

Aerosols play a crucial role in modifying the radiative properties of clouds, and aerosol-cloud interactions are the largest source of uncertainty in anthropogenic climate forcing (Forster et al., 2021). Our limited understanding of aerosol effects on clouds and Earth's climate impedes precise estimates of climate sensitivity to human-induced radiative forcing (Stevens et al., 2016), thereby reducing the reliability of future climate predictions. Cloud properties can be altered by aerosols in numerous ways, often depending on the environmental conditions under which the interaction occurs (Oreopoulos et al., 2020). By serving as cloud condensation nuclei (CCN), aerosols increase cloud droplet number concentration and decrease cloud droplet effective radius of liquid-water clouds, resulting in cloud brightening and thereby inducing a cooling effect on Earth's climate (Twomey, 1974). The net effect on cloud albedo also depends on aerosol-induced adjustments of cloud water, which can either enhance or partly offset this brightening (Toll et al., 2019; Trofimov et al., 2020). However, when anthropogenic aerosols act as ice-nucleating particles (INPs), they may promote glaciation of supercooled liquid-water clouds. Recent observational analysis by Toll et al. (2024) revealed glaciation of supercooled liquid-water clouds, snowfall, and reduced cloud cover near anthropogenic aerosol hot spots. Glaciation reduces the amount of solar radiation reflected back to space and could therefore contribute to warming if it is not limited to the immediate surroundings of anthropogenic aerosol hot spots (Toll et al., 2024).

Studies that rely on correlations between aerosol and cloud properties cannot definitively establish a causal link between aerosol concentrations and changes in the properties of clouds due to meteorological covariability (Liu et al., 2018; Stevens and Feingold, 2009; Quaas et al., 2020). The noise induced by meteorological covariability can be overcome by focusing on pollution sources within relatively pristine regions, where aerosol-polluted cloud tracks are identified in the middle of unpolluted cloud decks (Toll et al., 2019; Toll et al., 2024). As meteorological conditions are very similar between polluted areas downwind of aerosol hot spots and nearby unpolluted regions, and the level of aerosol pollution is the only major difference (Toll et al., 2019), CCN- and INP-induced cloud perturbations at anthropogenic air pollution hot spots enable to analyse the causal aerosol impacts on clouds across track-favouring meteorological conditions.

When an aerosol pollution hot spot is situated in a relatively pristine area, CCN-polluted clouds can form quasi-linear, ship-track-like polluted cloud lines (Toll et al., 2019; Trofimov et al., 2020). These CCN-induced perturbations stand out from the surrounding unpolluted cloud deck because they consist of more numerous and smaller cloud droplets. In this study, we refer to these aerosol-polluted cloud features as "CCN perturbations". Cloud perturbations linked to glaciation events appear with a similar shape and spatial extent to tracks, with a distinctive head pointing toward the aerosol source (Toll et al., 2024). However, whereas CCN perturbations appear brighter than their surroundings, glaciation-induced perturbations most often stand out as areas of reduced cloud cover. Here, we refer to these INP-induced perturbations as "INP perturbations". When no distinction between these mechanisms is made, we refer to both types of perturbations collectively as "events" or "event days".

https://doi.org/10.5194/egusphere-2026-6740
Preprint. Discussion started: 11 November 2026
© Author(s) 2026. CC BY 4.0 License.

The studied pollution sources are presumed to emit aerosol particles continuously; however, CCN and INP perturbations are observed only under specific meteorological conditions (Trofimov et al., 2022; Rahu et al., 2022). The primary objective of this study is to compare the meteorological conditions that favour the formation of CCN perturbations to those that lead to the development of INP perturbations. While aerosol properties determine whether particles can act as CCN or INPs (Hoose and Möhler, 2012), the surrounding atmospheric conditions strongly modulate whether aerosols lead to visible cloud perturbations (Gryspeerdt et al., 2021; Trofimov et al., 2022; Rahu et al., 2022).

Trofimov et al. (2022) and Rahu et al. (2022) found that conditions favouring CCN perturbations are predominantly controlled by synoptic-scale atmospheric circulation. Favourable conditions include clean air (low cloud droplet number concentrations), thin clouds and dry, statically stable atmospheric conditions, which were most commonly associated with synoptic-scale high-pressure patterns. These findings were further supported by Toll and Rahu (2023), who demonstrated that the mere presence of liquid-phase clouds is insufficient for CCN perturbations to form. While CCN perturbations occasionally appear shortly after cloud formation, they most often develop after the cloud has persisted for more than half an hour (Toll and Rahu, 2023). This highlights the importance of specific meteorological conditions, with diurnal cycles potentially playing a significant role in the formation of CCN perturbations. Toll et al. (2024) found that anthropogenic INP perturbations on clouds generally form under meteorological conditions similar to but colder than those favouring CCN perturbations.

Building on these findings, this study focuses on the aerosol sources previously analysed by Toll et al. (2024) while adopting the methodological framework of Trofimov et al. (2022). By visually identifying CCN and INP perturbations in Moderate Resolution Imaging Spectroradiometer (MODIS) satellite images and systematically comparing meteorological conditions on days with CCN-induced and INP-induced cloud perturbations, we aim to improve the understanding of how meteorological conditions modulate their formation.

2 Methods

We analysed aerosol-induced cloud perturbations at five sites: Cherepovets, Fokino and Volsk situated in Russia and Rouyn-Noranda (hereafter Noranda) and Regina situated in Canada (Table 1). For each site, each day from 2000 to the end of 2021 was assigned to one of four following categories (Fig. 1): (a) *zero day* – no liquid-phase clouds present; (b) *only-cloud day* – liquid-phase clouds present but no visually discernible pollution signal; (c) *INP perturbation day*; or (d) *CCN perturbation day*. Classification was performed by visual interpretation of imagery accessed via NASA's Global Imagery Browse Services (GIBS). We used Terra MODIS false-colour composite based on channels 3 (0.459–0.479 µm), 6 (1.628–1.652 µm) and 7 (2.105–2.155 µm). In this composite, liquid-water clouds appear white to peach, with larger droplets giving a more peach-coloured appearance, whereas ice clouds and snow- or ice-covered surfaces appear red to orange, because ice absorbs strongly in the shortwave-infrared channels (Fig. 1). CCN perturbations were identified as track-like features originating at or near the

https://doi.org/10.5194/egusphere-2026-6740
Preprint. Discussion started: 11 November 2026
© Author(s) 2026. CC BY 4.0 License.

aerosol source that appear whiter than the surrounding liquid-water cloud deck, indicating smaller cloud droplets in the polluted area (Fig. 1d). INP perturbations were identified as track-shaped cloud-free areas originating at or near the aerosol source within liquid-water cloud deck, often with a distinct head pointing towards the aerosol source (Fig. 1c; Toll et al., 2024). As aerosol properties are not measured in this study, the days are classified solely by the visible signature of the cloud response in close proximity to the aerosol source. Since we used only Terra MODIS satellite data, some perturbations forming after Terra satellite overpass time may have gone undetected.

Table 1: Description of the study sites used in the analysis. The expected aerosol components are inferred from the source type and the cited literature; aerosol composition was not measured during the analysed events

Site of study	Coordinates	Approximate overpass time of Terra satellite (UTC)	Elevation above sea level (m)	Main source of air pollution	Expected main aerosol components (inferred from source type)
Cherepovets	59°07′ N 37°54′ E	09:00	130	Processes of iron and steel production	Sulphate and iron-oxide-rich particles (Hleis et al., 2013; Vodyanitskii and Savichev, 2017)
Fokino	53°12′ N 34°25′ E	09:00	190	Cement production	Ca-rich mineral dust (CaO, $CaCO_3$); little SO_2 (U.S. EPA, 2022; Ivanov et al., 2018)
Noranda	48°14′ N 79°01′ W	16:00	310	The smelting of copper	Metal-bearing (e.g., Cu, Zn, Fe) sulphide and sulphate particles (Zdanowicz et al., 2006)
Regina	50°27′ N 104°36′ W	18:00	580	Oil refining	Sulphate and minor primary particles such as catalyst fines (Moreno et al., 2008)
Volsk	52°03′ N 47°23′ E	08:00	90	Cement production	Ca-rich mineral dust (CaO, $CaCO_3$); little SO_2 (U.S. EPA, 2022)

https://doi.org/10.5194/egusphere-2026-6740
Preprint. Discussion started: 11 November 2026
© Author(s) 2026. CC BY 4.0 License.

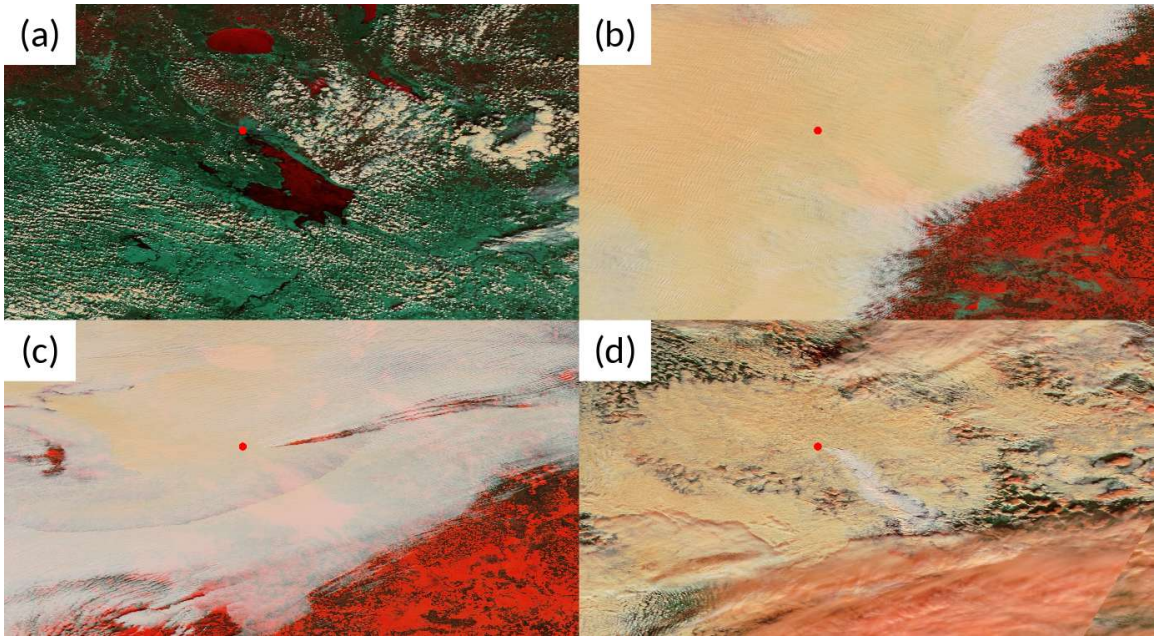


Figure 1: Examples of the four types of days used in this study. Examples are for the area surrounding Cherepovets, Russia, marked with a red dot in each image. (a) Zero day, with no suitable liquid-phase cloud present; (b) only-cloud day, with liquid-phase clouds present but no visually identifiable pollution signal; (c) INP-induced cloud perturbation day; and (d) CCN-induced cloud perturbation day.

We used the day-by-day classification to assess how meteorology influences whether aerosols serve as CCN and visibly brighten clouds or aerosols serve as INPs and promote glaciation. Furthermore, we compare the meteorological conditions across the four types of days. We compiled meteorological and cloud-property data from two data sources (Table 2): ERA5 reanalysis (Hersbach et al., 2020) and MODIS cloud products (Platnick et al., 2017).

From MODIS Level-3 data, we extracted six cloud properties for an approximately 150 km × 150 km area centred on each site (Table 2). Cloud properties were derived using the standard 2.1 μm MODIS retrieval algorithm (Platnick et al., 2017). From ERA5, we analysed selected pressure-level and single-level meteorological variables (Table 2). ERA5 variables were extracted at the time closest to the Terra satellite overpass (Table 1). Lower-tropospheric stability (LTS) was computed as (Klein and Hartmann, 1993), but with a modified lower-boundary term to better account for sites located above sea level. Because the 1000 hPa pressure level can lie below the surface at elevated locations, we replaced temperature at 1000 hPa with near-surface temperature:

https://doi.org/10.5194/egusphere-2026-6740
Preprint. Discussion started: 11 November 2026
© Author(s) 2026. CC BY 4.0 License.

$$LTS = T_{700} \cdot \left(\frac{1000}{700}\right)^{0.286} - T_{2m} \cdot \left(\frac{1000}{p_s}\right)^{0.286} \quad (1)$$

where T_{700} and T_{2m} refer to temperatures at the 700 hPa level and 2 metres above ground, and p_s is surface pressure.

Synoptic-scale atmospheric circulation was characterised using Jenkinson–Collison types (JCT; Jenkinson and Collison, 1977), computed from ERA5 850 hPa geopotential height fields with cost733class software (Philipp et al., 2016), following Trofimov et al. (2022). The method classifies each day into one of ten circulation classes based on the relative magnitudes of the resultant air flow (F) and vorticity (Z). When $F > |Z|$, the flow is treated as predominantly straight and assigned to one of eight directional types (N, NE, E, SE, S, SW, W, NW) according to flow direction. When $|Z| \geq F$, the circulation is classified as cyclonic (C; $Z > 0$) or anticyclonic (A; $Z < 0$) based on the sign of vorticity.

Anomalies were computed for all analysed variables relative to a climatological baseline. For each event, the climatological mean was defined as the average value for the same day of year and hour of day, based on the reference period 2000–2021. Alternative climatological definitions (e.g., including adjacent hours or days) yielded qualitatively similar results. Anomalies were then calculated as the difference between the event-day value and the corresponding climatological mean.

Unless stated otherwise, results are presented pooled across sites because the site-specific differences between CCN and INP perturbation days were qualitatively similar, even though event frequencies differed. The site-specific results are provided in the Supplement.

Table 2: Analysed meteorological variables and cloud properties.

ERA5 reanalysis single-level variables	ERA5 reanalysis variables on 500, 700, 1000 hPa pressure levels	MODIS
2 m dewpoint temperature	Relative humidity	Cloud droplet effective radius
2 m temperature	Vertical velocity	Cloud fraction
Zero degree level	U component of wind	Cloud optical thickness
Evaporation	V component of wind	Cloud top pressure
Boundary layer height	Temperature	Cloud top temperature
Total precipitation	Geopotential	Liquid water path
Cloud base height	Potential vorticity	
Mean sea level pressure	Vorticity	
10 m u component of wind	*Derived variables:*	
10 m v component of wind	Lower-tropospheric stability (from temperature and surface pressure)	
Surface pressure		

https://doi.org/10.5194/egusphere-2026-6740
Preprint. Discussion started: 11 November 2026
© Author(s) 2026. CC BY 4.0 License.

ERA5 reanalysis single-level variables	ERA5 reanalysis variables on 500, 700, 1000 hPa pressure levels	MODIS
10 m u component of neutral wind 10 m v component of neutral wind Convective available potential energy *Derived variables:* Wind speed, wind direction (from wind u, v components)	Wind speed, wind direction (from wind u,v components)	

3 Results

The occurrence of visible aerosol perturbations varied between the study sites. At Volsk, 52 INP perturbation days but no CCN perturbation days were identified among 1064 liquid-cloud days (Table 3). Because this prevents a comparison of CCN and INP perturbations at that site, Volsk is excluded from all subsequent analyses, and the results below refer to the four remaining sites.

Out of all days with liquid-phase clouds**,** only-cloud days were most common (662 cases), followed by days with CCN perturbations (469) and INP perturbations (303) (Table 3). Relative to all liquid-cloud days (N = 1434), CCN perturbations accounted for ~33 % and INP perturbations for ~21 % of cases. Across the study sites, liquid-phase clouds occurred on 3–7 % of all days. Among days with liquid-phase clouds, event days (CCN or INP perturbation days) comprised 36–68 %, corresponding to 1–5 % of all days.

Table 3: Occurrence frequencies of all four types of days as used in this study (Fig. 1).

	Total number of days 2000–2021				Percentages		
	Zero days (Z)	Only-cloud days (O)	CCN perturbation days (C)	INP perturbation days (I)	$\frac{O+C+I}{O+C+I+Z}$	$\frac{C+I}{O+C+I}$	$\frac{C+I}{O+C+I+Z}$
Cherepovets	7494	173	319	50	7 %	68 %	5 %
Fokino	7707	212	28	89	4 %	36 %	1 %
Noranda	7679	197	57	103	4 %	45 %	2 %
Regina	7830	80	65	61	3 %	61 %	2 %
Volsk	6972	1012	0	52	13 %	5 %	0.6 %
All sites combined (except Volsk)	30710	662	469	303	4 %	54 %	2 %

The occurrence frequencies of all three liquid-cloud categories (only-clouds, CCN perturbations and INP perturbations) exhibit strong seasonality (Fig. 2). Only-cloud days are concentrated in the cold season, with minima in summer. CCN perturbations occur year-round but peak sharply in autumn (September–November), whereas INP perturbations are almost exclusively a

https://doi.org/10.5194/egusphere-2026-6740
Preprint. Discussion started: 11 November 2026
© Author(s) 2026. CC BY 4.0 License.

cold-season phenomenon, with the largest number of cases in winter (November–February) and near-zero occurrence from late spring through early autumn.

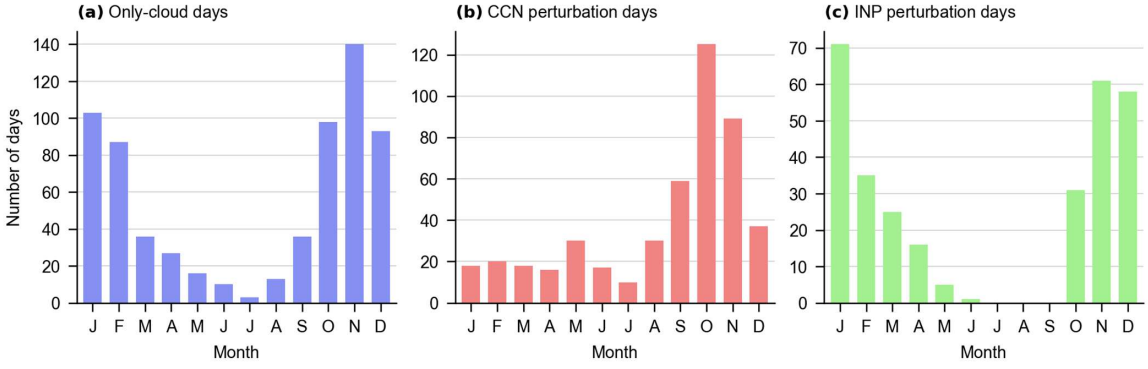
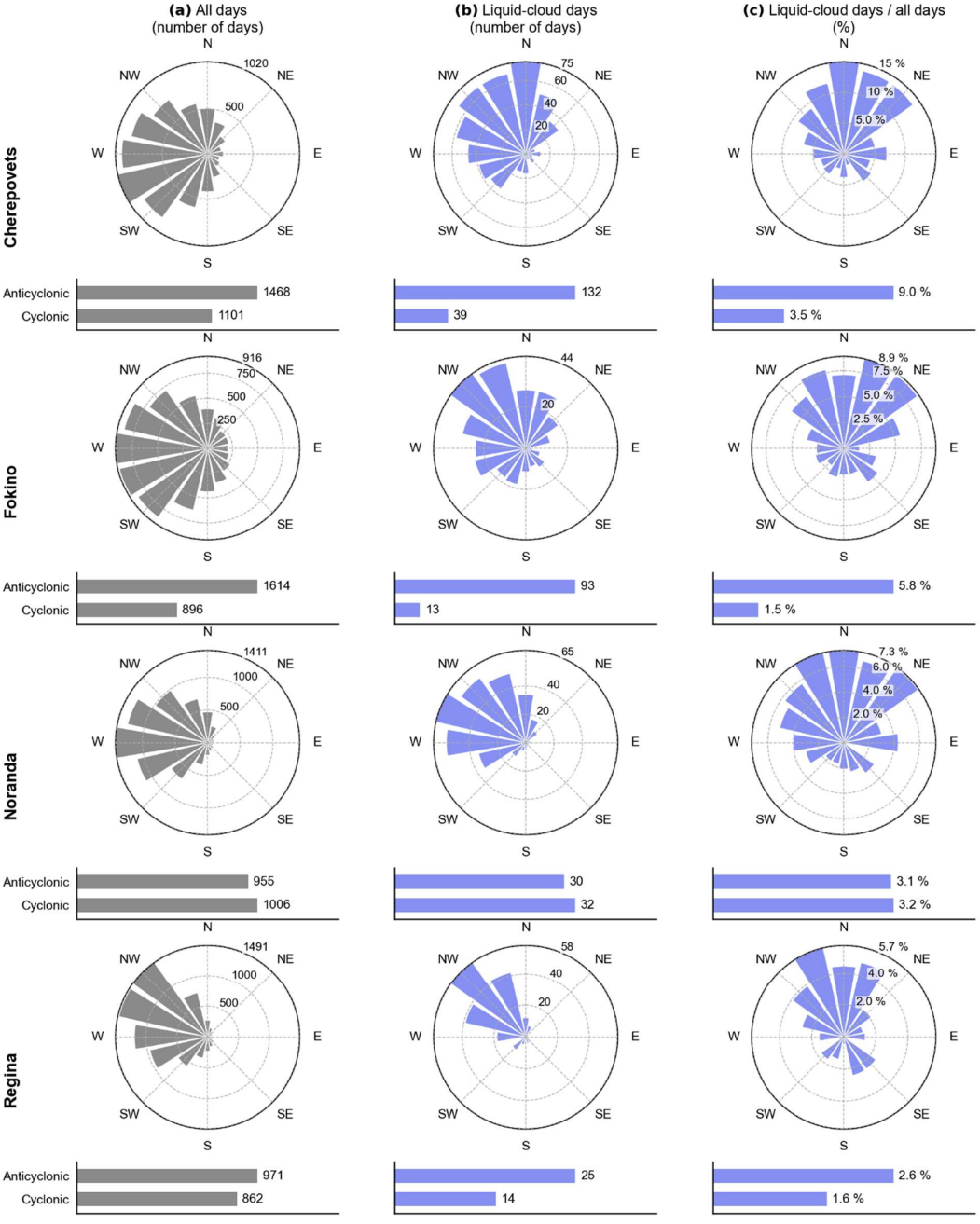


Figure 2: Monthly number of (a) only-cloud days, (b) CCN perturbation days and (c) INP perturbation days at the four analysed sites combined, 2000–2021.

The occurrence of liquid-phase clouds at the four analysed sites is strongly modulated by synoptic-scale circulation patterns (Fig. 3). Across all four sites, the prevailing synoptic-scale flow is generally westerly, although the dominant directional sector differs by location. South-westerly flow is most frequent in Cherepovets and Fokino, whereas north-westerly flow dominates in Regina. In the JCT classification, cyclonic and anticyclonic days occur in broadly similar proportions at most sites, except in Fokino, where anticyclonic conditions are nearly twice as frequent as cyclonic conditions (Fig. 3a).

Liquid-cloud days are shifted toward more northerly flow relative to the distribution across all days (the wind roses in Fig. 3b versus Fig. 3a). Liquid-cloud days are also more often anticyclonic than cyclonic at most sites, except in Noranda, where cyclonic and anticyclonic days occur in near-equal proportions (Fig. 3b). The clockwise shift toward northerly/easterly sectors appears again across all sites when moving from absolute day numbers to probability (the wind roses in Fig. 3c versus Fig. 3b). These easterly flow types are relatively rare overall, but when they do occur, they are comparatively favourable for liquid-phase cloud occurrence. For the cyclonic and anticyclonic classification, the probability distribution broadly follows the absolute day numbers distribution, with anticyclonic conditions remaining more favourable at most sites, while Noranda again shows little difference between the two circulation types (the cyclonic/anticyclonic bars in Fig. 3c versus Fig. 3b).

https://doi.org/10.5194/egusphere-2026-6740
Preprint. Discussion started: 11 November 2026
© Author(s) 2026. CC BY 4.0 License.



https://doi.org/10.5194/egusphere-2026-6740
Preprint. Discussion started: 11 November 2026
© Author(s) 2026. CC BY 4.0 License.

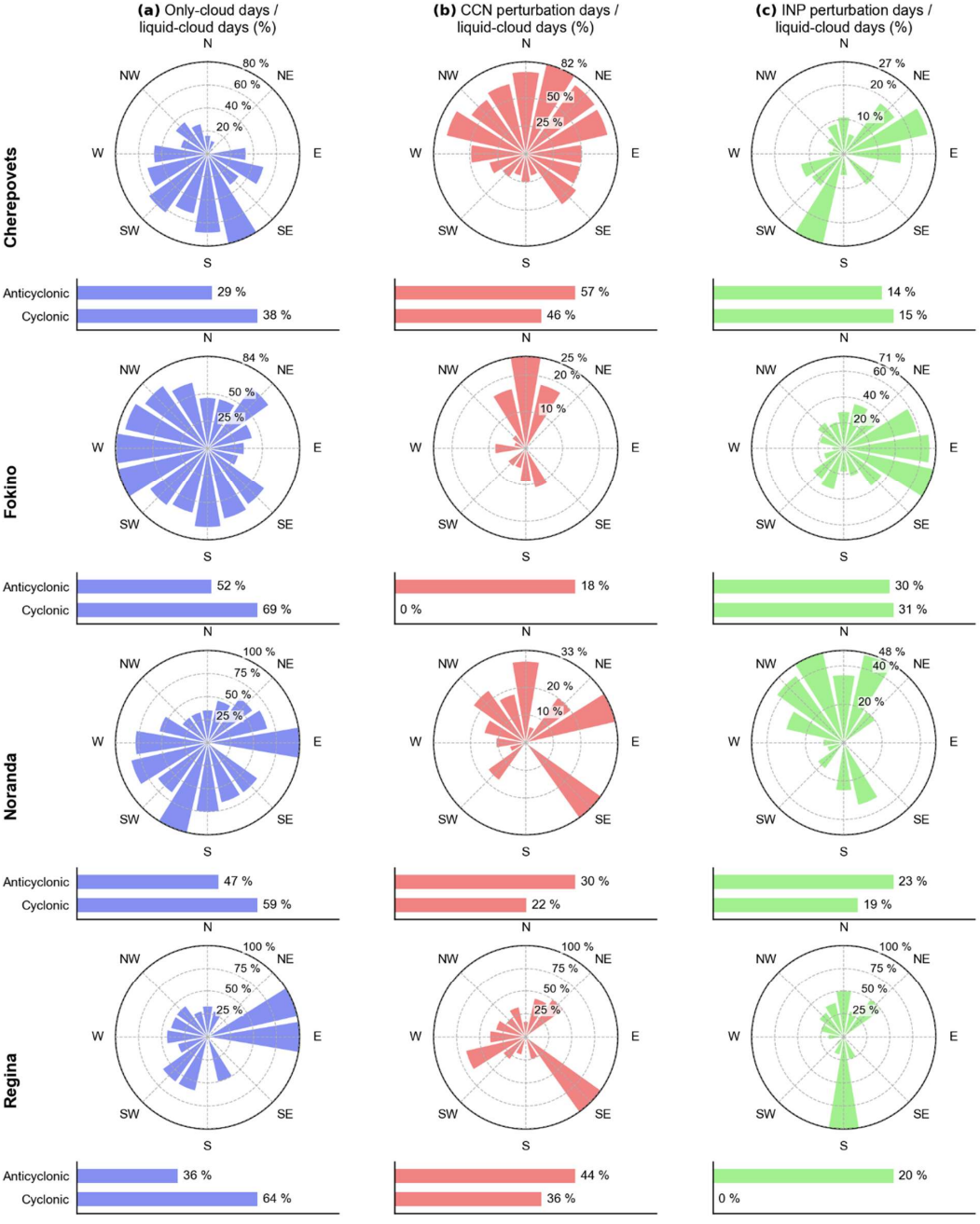
Figure 3: Frequency distributions of circulation types at the four analysed sites. Columns show (a) the number of all days, (b) the number of days with liquid-phase clouds, and (c) the probability of liquid-phase cloud occurrence, expressed as the percentage of all days within each circulation type that had liquid-phase clouds. In each panel, the wind roses show the distribution of ERA5 700 hPa wind direction and the bar charts below show the Jenkinson–Collison (JCT) cyclonic and anticyclonic types. The two are derived from different circulation classifications. Because the directional distributions from the two methods were very similar, only the ERA5-based directional distributions are shown, while bar charts show the additional JCT cyclonic and anticyclonic classes.

The likelihood of an only-cloud day or a CCN/INP perturbation varies systematically with circulation type when liquid-phase clouds are present (Fig. 4). At some sites, the signal is very clear. In Cherepovets, when liquid-phase clouds occur under westerly to south-easterly flow, the probability of an only-cloud day varies between about 60 % and 80 % depending on the specific wind sector, whereas under north-westerly to north-easterly flow, the probability of a CCN perturbation is about 60–80 %. INP perturbations are less common in Cherepovets, but under north-easterly or south-westerly flow, they still reach a probability of roughly 30 %, conditional on liquid-phase clouds being present. In the JCT classification, more than half of anticyclonic liquid-cloud days in Cherepovets are associated with CCN perturbations, whereas 38 % of cyclonic liquid-cloud days show no visible pollution signal. INP perturbations have similarly low probabilities under both cyclonic and anticyclonic conditions.

Equally strong but different patterns appear at other sites. In Fokino, easterly flow is associated with about a 70 % probability of INP perturbation formation when liquid-phase clouds are present, whereas no CCN perturbations occur under cyclonic conditions. Westerly flow is associated with more than 80 % probability of only-cloud days, and cyclonic days with liquid-phase clouds are associated with about 70 % probability of no visible pollution signal. In Noranda and Regina, by contrast, easterly flow is more strongly associated with only-cloud days, although some CCN perturbations still occur under north-easterly or south-easterly flow.

Across all sites, only-cloud days tend to be more closely associated with cyclonic conditions. Depending on the studied site, the event days are generally more frequent under anticyclonic conditions or show little difference between cyclonic and anticyclonic regimes.

https://doi.org/10.5194/egusphere-2026-6740
Preprint. Discussion started: 11 November 2026
© Author(s) 2026. CC BY 4.0 License.



https://doi.org/10.5194/egusphere-2026-6740
Preprint. Discussion started: 11 November 2026
© Author(s) 2026. CC BY 4.0 License.

Figure 4: Conditional likelihood of different liquid-cloud day types under different circulation conditions at the four analysed sites. Columns show the percentage of (a) only-cloud days, (b) CCN perturbation days, and (c) INP perturbation days among all liquid-cloud days within each circulation type, so that the values in (a)–(c) sum to 100 % for each circulation type. In each panel, the wind roses show the ERA5 700 hPa wind-direction distribution and the bar charts below show the JCT cyclonic and anticyclonic types. The two are based on different circulation classifications. The directional distributions derived from the JCT method were very similar to the ERA5-based distributions and are therefore not shown separately.

Meteorological conditions on CCN and INP perturbation days differ clearly in absolute terms, whereas differences in anomalies relative to the 2000–2021 climatology are mostly smaller (Table 4). Because CCN and INP perturbations predominantly occur at different times of the year, many absolute differences partly reflect seasonality; differences in anomalies remove this seasonal effect and therefore help identify variables more directly associated with the physical distinction between the two perturbation types. The p-values in Table 4 indicate the strength of statistical evidence for a difference in mean values; the limitations of this statistical test are considered in the discussion of the results.

Table 4: Mean absolute values and mean departures from climatology (2000–2021) for meteorological and cloud variables on CCN and INP perturbation days. For columns reporting differences between INP-day and CCN-day values, values in parentheses give the p-value from Welch's two-sample t-test for unequal variances, calculated between the corresponding distributions. For each event, the climatological mean was defined as the average value for the same day of year and hour of day, based on the reference period 2000–2021. Departure from climatology was then calculated as the difference between the event-day value and the corresponding climatological mean.

Meteorological variable	Mean value on INP perturbation days (a)	Mean value on CCN perturbation days (b)	a - b	Mean departure from climatology on INP perturbation days (c)	Mean departure from climatology on CCN perturbation days (d)	c - d
			Thermodynamic environment			
Temperature at 2 m (K)	267	277	-10 (10^{-98})	-3	-2	-1 (0.02)
Temperature at 700 hPa (K)	258	265	-7 (10^{-55})	-2	-1	-1 (10^{-5})
Zero-degree level (m)	76	1008	-932 (10^{-55})	-423	-290	-134 (10^{-3})
Cloud top temperature (K)	257	263	-6 (10^{-40})	5	6	-1 (10^{-3})
			Boundary-layer and cloud-regime structure			
Lower-tropospheric stability (K)	18	16	2 (10^{-9})	1	2	-1 (0.02)
Boundary layer height (m)	705	848	-143 (10^{-7})	107	87	20 (0.288)

https://doi.org/10.5194/egusphere-2026-6740
Preprint. Discussion started: 11 November 2026
© Author(s) 2026. CC BY 4.0 License.

Meteorological variable	Mean value on INP perturbation days (a)	Mean value on CCN perturbation days (b)	a - b	Mean departure from climatology on INP perturbation days (c)	Mean departure from climatology on CCN perturbation days (d)	c - d
Convective available potential energy (J kg^{-1})	4	6	-2 (0.027)	-1	-20	19 (10^{-10})
Cloud base height (m)	510	596	-86 (0.062)	-388	-356	-32 (0.546)
Synoptic and dynamical conditions						
Mean sea level pressure (hPa)	1024	1020	4 (10^{-7})	7	5	2 (10^{-3})
Vertical velocity at 1000 hPa (Pa s^{-1})	-0.01	0.01	-0.02 (10^{-14})	0.01	0.02	-0.02 (10^{-12})
Geopotential at 700 hPa (m^2 s^{-2})	28702	29275	-573 (10^{-18})	174	184	-10 (0.879)
Moisture conditions						
Dew point temperature at 2 m (K)	263	273	-10 (10^{-105})	-2	-1	-1 (10^{-5})
Relative humidity at 700 hPa (%)	40	36	4 (0.039)	-18	-20	2 (0.114)
Wind field						
Wind direction at 700 hPa (°)	235	215	20 (0.031)	-5	-19	14 (0.108)
Wind velocity at 10 m (m s^{-1})	3	4	-1 (10^{-4})	-1	0	-1 (0.011)
Cloud properties						
Cloud water path (g m^{-2})	169	158	11 (0.240)	-148	-81	-67 (10^{-8})
Cloud optical thickness (1)	27	23	4 (10^{-3})	-13	-9	-4 (10^{-3})
Cloud fraction (%)	96	95	1 (0.401)	15	17	-2 (0.02)
Cloud droplet effective radius (μm)	11	12	-1 (10^{-6})	-3	-1	-2 (10^{-10})

INP perturbations occur in a distinctly colder environment than CCN perturbations, and this remains true even after accounting for seasonality (Table 4; Fig. 5a, b). INP perturbations also occur under slightly higher mean sea level pressure (MSLP) than CCN perturbations, both in absolute values and relative to the 2000-2021 climatology (Table 4). In absolute terms, INP perturbations form in a statically more stable atmosphere with more shallow boundary layer, compared to CCN perturbations (Fig. 5c; Table 4), but this difference is reversed when comparison is carried out relative to the background climatology (Fig.

https://doi.org/10.5194/egusphere-2026-6740
Preprint. Discussion started: 11 November 2026
© Author(s) 2026. CC BY 4.0 License.



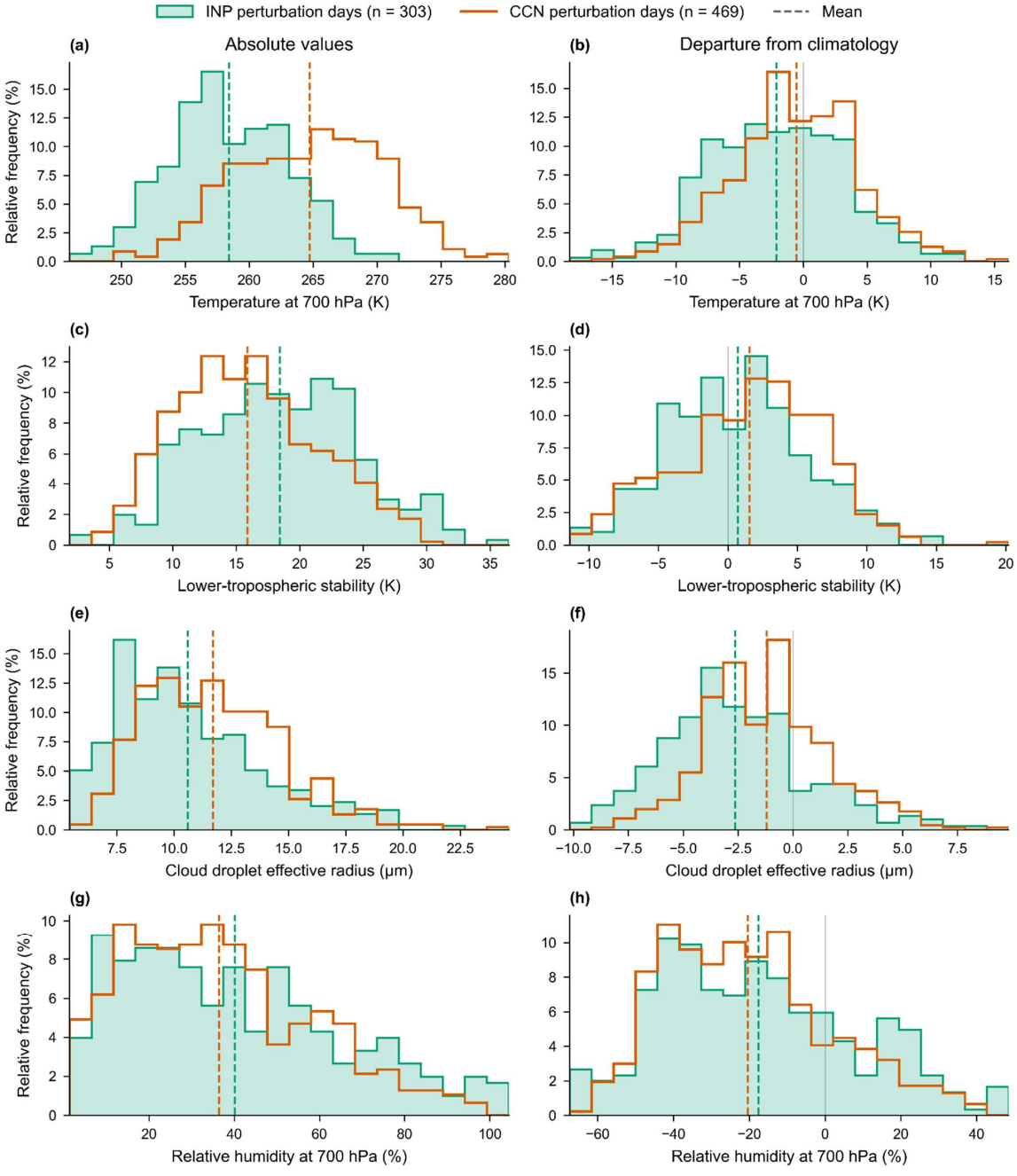
5d; Table 4). INP perturbations are associated with smaller cloud droplet effective radii than CCN perturbations, both in absolute values and relative to climatology (Fig. 5e, f). While both INP and CCN perturbations form on days with low relative humidity, INP perturbations tend to occur under slightly moister conditions in absolute terms; but relative to climatology, this

https://doi.org/10.5194/egusphere-2026-6740
Preprint. Discussion started: 11 November 2026
© Author(s) 2026. CC BY 4.0 License.



difference is not significant (Fig. 5g, h). INP perturbations are associated with weak large-scale ascent at 1000 hPa, whereas CCN perturbations are associated with weak descent (Table 4).

https://doi.org/10.5194/egusphere-2026-6740
Preprint. Discussion started: 11 November 2026
© Author(s) 2026. CC BY 4.0 License.



https://doi.org/10.5194/egusphere-2026-6740
Preprint. Discussion started: 11 November 2026
© Author(s) 2026. CC BY 4.0 License.

Figure 5: Distributions of (a, b) temperature at 700 hPa, (c, d) lower-tropospheric stability, (e, f) cloud droplet effective radius and (g, h) relative humidity at 700 hPa on days with INP perturbations (green, filled) and CCN perturbations (red, outline) at the four analysed sites. The left column shows absolute event-day values and the right column departures from climatology, defined as the event-day value minus the climatological mean for the same day of year and hour of day. Histograms show the percentage of days of each type per bin; dashed lines mark the mean values.

4 Discussion and conclusions

This study extends earlier research on ship-track like natural experiments (CCN-induced cloud perturbations) (Trofimov et al., 2022) by explicitly comparing the meteorological conditions associated with visible CCN and INP perturbations on clouds at industrial aerosol hot spots. Relative to climatology, both CCN and INP perturbations occur under higher-than-normal sea level pressure and dry air at 700 hPa. In absolute terms, the CCN- and INP-favouring meteorological conditions differ most clearly in temperature, and most other absolute differences largely reflect the different seasonal occurrence of CCN and INP perturbations. Once seasonality is accounted for, the remaining differences are mostly small, and several of them lack a clear physical interpretation. Extending the findings of Trofimov et al. (2022), we thus show that conditions previously identified as favouring CCN perturbations – dry and statically relatively stable environments under high air pressure conditions – are also associated with INP perturbations.

In Volsk, we observed INP perturbations but no CCN perturbations, and at sites where both signals occur, the CCN-to-INP perturbation ratio still differs strongly from place to place. Differences in the chemical composition of the emitted aerosol offer a plausible explanation for these contrasts. Volsk is a cement-production hot spot and is therefore expected to emit calcium-rich mineral dust (Ivanov et al., 2018). Fine-mode sulphate, typical for sulphur-rich industrial sources, is likely less important there, because the highly alkaline environment of cement kilns absorbs about 70 % to more than 95 % of the SO_2 released (U.S. EPA, 2022). Mineral dust is among the most important and efficient atmospheric INP types, while its CCN effectiveness is often limited by relatively low hygroscopicity compared with salts such as sulphate (Kanji et al., 2017). It is important to note that “no visible tracks” is not equivalent to “no CCN effect.” Aerosol emissions can measurably alter cloud microphysics even when no perturbation is visible (Manshausen et al., 2022), implying that Volsk could still have CCN-driven changes in cloud properties that simply do not meet the visibility threshold of our manual classification approach.

Since the absence of visible CCN perturbations at Volsk currently prevents CCN–INP perturbation comparisons at that site, we excluded Volsk from the main analyses under the results section. Across the remaining sites, Cherepovets, where the integrated iron and steel works are expected to emit iron-oxide-rich primary particles (Hleis et al., 2013; Vodyanitskii and Savichev, 2017) together with SO_2, shows far more frequent CCN perturbations. Fokino, where calcium-rich cement dust is likely the main aerosol component, as in Volsk (Ivanov et al., 2018), and Noranda, where the smelter plume is rich in metal-bearing sulphide and sulphate particles (Zdanowicz et al., 2006), show more frequent INP perturbations. In Regina, where

https://doi.org/10.5194/egusphere-2026-6740
Preprint. Discussion started: 11 November 2026
© Author(s) 2026. CC BY 4.0 License.

refinery emissions are expected to consist mainly of SO_2, with minor primary particles such as catalyst fines (Moreno et al., 2008), CCN and INP perturbations occur in nearly equal numbers. These differences indicate that aerosol source type alone does not uniquely determine the cloud response. Sources that produce sulphate-rich aerosols may also co-emit metal oxides, ash, or other mineral particles that can act as INPs, and Toll et al. (2024) reported five glaciation events even downwind of nuclear power plants.

It should be emphasised that the aerosol composition at each site is inferred from the source type and the literature cited in Table 1, rather than measured during the analysed events. The site-to-site differences in the relative frequency of CCN and INP perturbations are consistent with a strong influence of aerosol chemical composition on the dominating perturbation type, but demonstrating that the chemical composition is the primary controlling factor would require concurrent measurements of aerosol chemical composition, CCN, INP, and cloud properties.

Among meteorological variables, temperature is the clearest discriminator between CCN and INP perturbation events. In statistics pooled across all sites, INP perturbations occur on substantially colder days than CCN perturbations at both 2 m and 700 hPa, with a much lower zero-degree isotherm level, and this separation remains evident even when accounting for seasonality (Fig. 5a, b; Table 4). This result follows the basic microphysics, where the likelihood and the rate of heterogeneous ice nucleation increases rapidly with decreasing temperature (Hoose and Möhler, 2012; Kanji et al., 2017).

Circulation analysis indicates that synoptic-scale flow is strongly related to (i) whether suitable liquid-phase cloud exists and (ii) whether a visible pollution perturbation is present on those liquid-cloud days. However, circulation pattern provides less confident separation between CCN and INP perturbations (Fig. 3, 4). The direction of the synoptic-scale circulation can, in some cases, provide a rough indication of the likelihood of CCN perturbation formation, particularly when liquid-phase cloud is already present, whereas INP perturbations appear less strongly tied to any specific circulation patterns. Across all sites, liquid clouds were more likely to occur under flow patterns shifted clockwise from the most common airflows (Fig. 3). The circulation patterns associated with visually detectable aerosol perturbations, given that liquid clouds are present, appear to be more site-specific (Fig. 4). A high frequency of perturbations under a given circulation type can have several explanations: the circulation may favour the formation of liquid clouds, favour coupling between the aerosol pollution plume and the cloud layer, or favour conditions under which clouds are more susceptible to aerosol, such as cleaner air with larger cloud droplets. Our analysis cannot fully separate these effects.

In absolute terms, INP perturbations occur in statically more stable, shallower boundary-layer conditions than CCN perturbations; however, this contrast weakly reverses (by about 1 K for LTS) when considering anomalies relative to the seasonal baseline, suggesting that static stability and boundary layer height primarily reflect seasonality rather than event-specific physical controls. Trofimov et al. (2022) interpreted the lack of CCN perturbations under statically very stable conditions as a vertical reach limit of pollution; however, as glaciation-type signals can occur under statically very stable, shallow boundary-layer regimes, then static stability alone cannot be treated as a simple limiting parameter that prevents

https://doi.org/10.5194/egusphere-2026-6740
Preprint. Discussion started: 11 November 2026
© Author(s) 2026. CC BY 4.0 License.

aerosol–cloud interactions. One plausible reason is that many industrial plumes are hot and buoyant and can inject aerosol above the shallow statically stable boundary layer (mean boundary layer height of about 700 m on INP perturbation days; Table 4), and Toll et al. (2024) explicitly discuss possibility of cases (including near nuclear power plants) where buoyant plumes may loft nearby aerosols that serve as INPs, emphasising that vertical coupling can occur even when near-surface static stability is very high.

The positive mean sea level pressure anomaly for both CCN and INP perturbations suggests that event days preferentially occur within higher-pressure synoptic environments even after accounting for seasonality, with slightly stronger anomalies for INP perturbations. This is broadly consistent with Trofimov et al. (2022), who interpreted high MSLP as "anticyclonic preference" for aerosol perturbations on clouds. However, our circulation classification shows that the preference for anticyclonic over cyclonic conditions is weak and therefore does not clearly discriminate between CCN and INP perturbations. From a dynamical perspective, higher-sealevel-pressure environments are commonly associated with large-scale descent. Vertical velocity is relevant because it regulates supersaturation and therefore the fraction of aerosol that activates as cloud condensation nuclei, particularly in regimes where activation is updraught-limited (Peng et al., 2005). However, neither the anticyclonic preference interpretation nor the role of large-scale descent in regulating aerosol activation fully explains why INP perturbations occur on days with higher MSLP than CCN perturbations. Despite their higher average MSLP, INP perturbations are associated with weaker large-scale descent than CCN perturbations (Table 4) and show a less pronounced preference for anticyclonic over cyclonic conditions (Fig. 4). The higher MSLP values on days with INP perturbations therefore cannot be straightforwardly interpreted as a stronger anticyclonic or subsidence signal. One possible explanation is seasonality: INP perturbations occur more frequently in winter, when air pressure can be higher, even if this does not necessarily translate into a stronger anticyclonic-flow signature in the circulation classification. Yet the slightly larger positive MSLP anomalies during INP perturbations persist even after the seasonal cycle is removed.

A particularly robust feature is that both CCN and INP perturbations occur on days with low relative humidity on all analysed pressure levels, most strikingly at 700 hPa (RH700) – as also found for CCN perturbations by Trofimov et al. (2022), even though INP perturbations occur under slightly moister conditions than CCN perturbations in absolute terms (Fig. 5g). This is not easily dismissed as seasonality because the RH signal persists in departures from climatology. Drier air can enhance cloud-top radiative cooling and strengthen in-cloud updraughts (Zheng et al., 2016), increasing cloud susceptibility to aerosol perturbations (Twomey, 1959) and potentially contributing to the observed dependence of track formation on relative humidity (Gryspeerdt et al., 2019). It is less clear why RH700 should affect INP perturbations less than CCN perturbations, but this difference is small and likely cannot be used as a discriminator.

Several limitations should be considered when interpreting the statistical comparisons. The p-values in Table 4 should be interpreted with caution because consecutive event days may not be independent. Individual weather systems and associated perturbations can persist for several days (Toll and Rahu, 2023), while the meteorological conditions driving a perturbation

https://doi.org/10.5194/egusphere-2026-6740
Preprint. Discussion started: 11 November 2026
© Author(s) 2026. CC BY 4.0 License.

may already be present before its observable onset. This temporal dependence violates the independence assumption of Welch's t-test (Welch, 1947). Moreover, p-values do not quantify the magnitude or physical importance of a difference (Wasserstein and Lazar, 2016). We nevertheless report them as a simple and reproducible indication of the statistical evidence for differences between the groups.

One limitation of visual classification is that the detectability of perturbations may depend on background cloud properties. CCN perturbations appear in clouds with larger droplets, while INP perturbations appear in smaller-droplet clouds (Fig. 5e). It could reflect detectability: brightening requires a sufficiently "clean" background cloud state to produce contrast in the false-colour imagery. The detection of INP perturbation is possible even when droplet sizes are already small because the main signature is the reduction in cloud cover. This highlights a limitation of visual classification and underscores the value of automated detection methods in future work. At the same time, for strong and unambiguous perturbations, manual detection provides a robust reference and can serve as a benchmark for validating automated approaches. Automated approaches could then apply consistent detection criteria for CCN and INP perturbations across different background cloud states, reduce observer-dependent bias, and help identify weaker or visually less obvious perturbations that may be missed in manual analysis.

Data availability

The lists of dates for CCN perturbations, INP perturbations, only-cloud days, and zero days for each study site are available at [will be filled later]. The RGB images (MODIS channels 3-6-7) used for the visual detection of polluted clouds from https://worldview.earthdata.nasa.gov/ were used. ERA5 hourly data were downloaded from Climate Data Store (CDS), from https://doi.org/10.24381/cds.adbb2d47 for single levels and from https://doi.org/10.24381/cds.bd0915c6 for pressure levels. The MODIS data were downloaded from https://giovanni.gsfc.nasa.gov/giovanni. The software cost733class for calculating circulation types was created during COST Action 733 "Harmonisation and Applications of Weather Types Classifications for European Regions," and we are grateful to its creators.

Author contributions

HT and VT designed the study. HT performed all the analysis. PP performed the calculations using the cost733class software. HT wrote the manuscript with the contributions from VT, PP, HK, JR, AL and MA.

Competing interests

The authors declare that they have no conflict of interest.

https://doi.org/10.5194/egusphere-2026-6740
Preprint. Discussion started: 11 November 2026
© Author(s) 2026. CC BY 4.0 License.

Financial support

This work was funded by Estonian Research Council grant No. PRG1726 and by European Research Council Consolidator Grant CloudTracker, with the project No 101230369.

References

Forster, P., Storelvmo, T., Armour, K., Collins, W., Dufresne, J.-L., Frame, D., Lunt, D. J., Mauritsen, T., Palmer, M. D., Watanabe, M., Wild, M., and Zhang, H.: The Earth's energy budget, climate feedbacks, and climate sensitivity, in: *Climate* Change *2021: The* Physical Science Basis*. Contribution of Working Group I to the Sixth Assessment Report of the Intergovernmental Panel on Climate Change*, edited by: Masson-Delmotte, V., Zhai, P., Pirani, A., Connors, S. L., Péan, C., Berger, S., Caud, N., Chen, Y., Goldfarb, L., Gomis, M. I., Huang, M., Leitzell, K., Lonnoy, E., Matthews, J. B. R., Maycock, T. K., Waterfield, T., Yelekçi, O., Yu, R., and Zhou, B., Cambridge University Press, 923–1054, https://doi.org/10.1017/9781009157896.009, 2021.

Gryspeerdt, E., Smith, T. W., O'Keeffe, E., Christensen, M. W., and Goldsworth, F. W.: The impact of ship emission controls recorded by cloud properties, Geophys. Res. Lett., 46, 12547–12555, https://doi.org/10.1029/2019GL084700, 2019.

Gryspeerdt, E., Goren, T., and Smith, T. W. P.: Observing the timescales of aerosol–cloud interactions in snapshot satellite images, Atmos. Chem. Phys*., 21*, 6093–6109, https://doi.org/10.5194/acp-21-6093-2021, 2021.

Hersbach, H., Bell, B., Berrisford, P., Hirahara, S., Horányi, A., Muñoz-Sabater, J., Nicolas, J., Peubey, C., Radu, R., Schepers, D., Simmons, A., Soci, C., Abdalla, S., Abellan, X., Balsamo, G., Bechtold, P., Biavati, G., Bidlot, J., Bonavita, M., De Chiara, G., Dahlgren, P., Dee, D., Diamantakis, M., Dragani, R., Flemming, J., Forbes, R., Fuentes, M., Geer, A., Haimberger, L., Healy, S., Hogan, R. J., Hólm, E., Janisková, M., Keeley, S., Laloyaux, P., Lopez, P., Lupu, C., Radnoti, G., de Rosnay, P., Rozum, I., Vamborg, F., Villaume, S., and Thépaut, J.-N.: The ERA5 global reanalysis, Q. J. Roy. Meteor. Soc., *146*, 1999–2049, https://doi.org/10.1002/qj.3803, 2020.

Hleis, D., Fernández-Olmo, I., Ledoux, F., Kfoury, A., Courcot, L., Desmonts, T., and Courcot, D.: Chemical profile identification of fugitive and confined particle emissions from an integrated iron and steelmaking plant, J. Hazard. Mater., 250–251, 246–255, https://doi.org/10.1016/j.jhazmat.2013.01.080, 2013.

Hoose, C. and Möhler, O.: Heterogeneous ice nucleation on atmospheric aerosols: A review of results from laboratory experiments, Atmos. Chem. Phys*., 12*, 9817–9854, https://doi.org/10.5194/acp-12-9817-2012, 2012.

Ivanov, Y. V., Kartashov, A. V., Ivanova, A. I., Ivanov, V. P., Marchenko, S. I., Nartov, D. I., and Kuznetsov, V. V.: Long-term impact of cement plant emissions on the elemental composition of both soils and pine stands and on the formation of Scots pine seeds, Environ. Pollut., 243, 1383–1393, https://doi.org/10.1016/j.envpol.2018.09.099, 2018.

https://doi.org/10.5194/egusphere-2026-6740
Preprint. Discussion started: 11 November 2026
© Author(s) 2026. CC BY 4.0 License.

Jenkinson, A. F. and Collison, F. P.: *An initial climatology of gales over the North Sea*, Synoptic Climatology Branch Memorandum No. 62, Meteorological Office, 1977.

Kanji, Z. A., Ladino, L. A., Wex, H., Boose, Y., Burkert-Kohn, M., Cziczo, D. J., and Krämer, M.: Overview of ice nucleating particles, Meteor. Monogr., 58, 1.1–1.33, https://doi.org/10.1175/AMSMONOGRAPHS-D-16-0006.1, 2017.

Klein, S. A. and Hartmann, D. L.: The seasonal cycle of low stratiform clouds, J. *Climate, 6*, 1587–1606, https://doi.org/10.1175/1520-0442(1993)006<1587:TSCOLS>2.0.CO;2, 1993.

Liu, Y., Zhang, J., Zhou, P., Lin, T., Hong, J., Shi, L., Yao, F., Wu, J., Guo, H., and de Leeuw, G.: Satellite-based estimate of the variability of warm cloud properties associated with aerosol and meteorological conditions, Atmos. Chem. Phys., *18*, 18187–18202, https://doi.org/10.5194/acp-18-18187-2018, 2018.

Manshausen, P., Watson-Parris, D., Christensen, M. W., Jalkanen, J.-P., and Stier, P.: Invisible ship tracks show large cloud sensitivity to aerosol, *Nature, 610*, 101–106, https://doi.org/10.1038/s41586-022-05122-0, 2022.

Moreno, T., Querol, X., Alastuey, A., and Gibbons, W.: Identification of FCC refinery atmospheric pollution events using lanthanoid- and vanadium-bearing aerosols, Atmos. Environ., 42, 7851–7861, https://doi.org/10.1016/j.atmosenv.2008.07.013, 2008.

Oreopoulos, L., Cho, N., and Lee, D.: A global survey of apparent aerosol-cloud interaction signals, J. Geophys. Res.-Atmos., *125*, e2019JD031287, https://doi.org/10.1029/2019JD031287, 2020.

Peng, Y., Lohmann, U., and Leaitch, R.: Importance of vertical velocity variations in the cloud droplet nucleation process of marine stratus clouds, J. Geophys. Res.-Atmos., *110*, D21209, https://doi.org/10.1029/2004JD004922, 2005.

Philipp, A., Beck, C., Huth, R., and Jacobeit, J.: Development and comparison of circulation type classifications using the COST 733 dataset and software, Int. J. Climatol., 36, 2673–2691, https://doi.org/10.1002/joc.3920, 2016.

Platnick, S., Meyer, K. G., King, M. D., Wind, G., Amarasinghe, N., Marchant, B., Arnold, G. T., Zhang, Z., Hubanks, P. A., Holz, R. E., Yang, P., Ridgway, W. L., and Riedi, J.: The MODIS cloud optical and microphysical products: Collection 6 updates and examples from Terra and Aqua, *IEEE* T. Geosci. *Remote, 55*, 502–525, https://doi.org/10.1109/TGRS.2016.2610522, 2017.

Quaas, J., Arola, A., Cairns, B., Christensen, M., Deneke, H., Ekman, A. M. L., Feingold, G., Fridlind, A., Gryspeerdt, E., Hasekamp, O., Li, Z., Lipponen, A., Ma, P.-L., Mülmenstädt, J., Nenes, A., Penner, J. E., Rosenfeld, D., Schrödner, R., Sinclair, K., Sourdeval, O., Stier, P., Tesche, M., van Diedenhoven, B., and Wendisch, M.: Constraining the Twomey effect from satellite observations: Issues and perspectives, Atmos. Chem. Phys., *20*, 15079–15099, https://doi.org/10.5194/acp-20-15079-2020, 2020.

Rahu, J., Trofimov, H., Post, P., and Toll, V.: Diurnal evolution of cloud water responses to aerosols, J. Geophys. Res.-Atmos., *127*, e2021JD035091, https://doi.org/10.1029/2021JD035091, 2022.

https://doi.org/10.5194/egusphere-2026-6740
Preprint. Discussion started: 11 November 2026
© Author(s) 2026. CC BY 4.0 License.



Stevens, B. and Feingold, G.: Untangling aerosol effects on clouds and precipitation in a buffered system, *Nature, 461*, 607–613, https://doi.org/10.1038/nature08281, 2009.

Stevens, B., Sherwood, S. C., Bony, S., and Webb, M. J.: Prospects for narrowing bounds on Earth's equilibrium climate sensitivity, *Earth's Future, 4*, 512–522, https://doi.org/10.1002/2016EF000376, 2016.

Toll, V. and Rahu, J.: Strong anthropogenic cloud perturbations can persist for multiple days, J. Geophys. Res.-Atmos., 128, e2022JD038146, https://doi.org/10.1029/2022JD038146, 2023.

Toll, V., Christensen, M., Quaas, J., and Bellouin, N.: Weak average liquid-cloud-water response to anthropogenic aerosols, Nature, 572, 51–55, https://doi.org/10.1038/s41586-019-1423-9, 2019.

Toll, V., Rahu, J., Keernik, H., Trofimov, H., Voormansik, T., Manshausen, P., Hung, E., Michelson, D., Christensen, M. W., Post, P., Junninen, H., Murray, B. J., Lohmann, U., Watson-Parris, D., Stier, P., Donaldson, N., Storelvmo, T., Kulmala, M., and Bellouin, N.: Glaciation of liquid clouds, snowfall, and reduced cloud cover at industrial aerosol hot spots, *Science, 386*, 756–762, https://doi.org/10.1126/science.adl0303, 2024.

Trofimov, H., Bellouin, N., and Toll, V.: Large-scale industrial cloud perturbations confirm bidirectional cloud water responses to anthropogenic aerosols, J. Geophys. Res.-Atmos., *125*, e2020JD032575, https://doi.org/10.1029/2020JD032575, 2020.

Trofimov, H., Post, P., Gryspeerdt, E., and Toll, V.: Meteorological conditions favorable for strong anthropogenic aerosol impacts on clouds, J. Geophys. Res.-Atmos., 127, e2021JD035871, https://doi.org/10.1029/2021JD035871, 2022.

Twomey, S.: The nuclei of natural cloud formation part II: The supersaturation in natural clouds and the variation of cloud droplet concentration, Geofis. Pura Appl., *43*, 243–249, https://doi.org/10.1007/BF01993560, 1959.

Twomey, S.: Pollution and the planetary albedo, Atmos. Environ., *8*, 1251–1256, https://doi.org/10.1016/0004-6981(74)90004-3, 1974.

US EPA: Portland cement manufacturing, Sect. 11.6, in: AP-42: Compilation of air emissions factors from stationary sources, 5th edn., Vol. I, US Environmental Protection Agency, https://www.epa.gov/system/files/documents/2022-03/c11s06_final.pdf, 2022.

Vodyanitskii, Y. N. and Savichev, A. T.: Magnetite contamination of urban soils in European Russia, Ann. Agrar. Sci., 15, 155–162, https://doi.org/10.1016/j.aasci.2017.05.020, 2017.

Wasserstein, R. L. and Lazar, N. A.: The ASA statement on p-values: Context, process, and purpose, Am. Stat., 70, 129–133, https://doi.org/10.1080/00031305.2016.1154108, 2016.

Welch, B. L.: The generalization of 'Student's' problem when several different population variances are involved, Biometrika, 34, 28–35, https://doi.org/10.1093/biomet/34.1-2.28, 1947.

Zdanowicz, C. M., Banic, C. M., Paktunc, D. A., and Kliza-Petelle, D. A.: Metal emissions from a Cu smelter, Rouyn-Noranda, Québec: Characterization of particles sampled in air and snow, Geochem.-Explor. Env. Anal., *6*, 147–162, https://doi.org/10.1144/1467-7873/05-089, 2006.

https://doi.org/10.5194/egusphere-2026-6740
Preprint. Discussion started: 11 November 2026
© Author(s) 2026. CC BY 4.0 License.



Zheng, Y., Rosenfeld, D., and Li, Z.: Quantifying cloud base updraft speeds of marine stratocumulus from cloud top radiative cooling, Geophys. Res. Lett., 43, 11407–11413, https://doi.org/10.1002/2016GL071185, 2016.